RESEARCH ARTICLE

Octagon-embedded carbohelicene as chiral motif for CPL emission of saddle-helix nanographenes

Miguel A. Medel,[a] *Rubén Tapia,*[a] *Victor Blanco,*[a] *Delia Miguel,*[b] *Sara P. Morcillo**[a] *and Araceli G. Campaña**[a]

[a] M. A. Medel, Dr. R. Tapia, Dr. V. Blanco, Dr. S. P. Morcillo, Dr. A. G. Campaña
Departamento de Química Orgánica, Unidad de Excelencia de Química (UEQ). Facultad de Ciencias. Universidad de Granada. 18071 Granada (Spain)
E-mail: samorcillo@ugr.es, araceligc@ugr.es

[b] Dr. D. Miguel
Departamento de Fisicoquímica, Facultad de Farmacia, UEQ, Universidad de Granada, Granada, Spain

Supporting information for this article is given via a link at the end of the document. CCDC-2032602 contains the supplementary crystallographic data for this paper. These data can be obtained free of charge from The Cambridge Crystallographic Data Centre

Abstract: We report a new family of hexa-*peri*-hexabenzocoronene (HBC)-based helical nanographenes incorporating π-extended carbo[5]helicenes bearing an octagonal carbocycle. This family represents a new kind of highly distorted saddle-helix hybrid nanographenes. For the first time, the eight-membered ring becomes a constituent of both a carbo[5]helicene and a HBC and thus, the negative curvature is responsible for twisting both units. This novel chiral motif, namely, *oct-[5]helicene* results in the largest torsion angle recorded so far for a carbo[5]helicene (θ=89.5º), as it has been suggested by DFT-calculations and confirmed by X-ray crystallography. Consequently, the barriers of isomerization become exceptionally high for a [5]helicene unsubstituted in the fjord region since neither racemization nor decomposition were observed at 200 ºC for **1** or **3** during 5h. Therefore, racemic resolutions allowed subsequent chiroptical studies showing the ECD and CPL responses of this novel family of chiral nanographenes.

Introduction

The chemistry of making non-planar carbon-based aromatic systems[1] is attracting growing interest not only for their capability to modify and enhance the electronic and optical properties of their planar counterparts[2] but also to discover novel chiroptical properties of interest in a variety of applications.[3] A prerequisite for making them valuable as chiral materials in organic electronics[4] is to reach stereochemically rigid structures, thus avoiding racemization processes. However, strategies to reach rigid curved polycyclic aromatic hydrocarbons (PAHs) with enough stiffness and stability to study their chiroptical properties become exceptionally challenging.[5] To date, creative synthetic methodologies have been used to isolate enantiopure helically twisted PAHs.[6] Among them, the incorporation of hexabenzocoronenes (HBCs) (Fig 1) into 3D scaffolds has emerged as an elegant strategy that enables the access to a new family of distorted nanographenes, the so-called "superhelicenes".[7]

Recently, a second approach has arisen for the study of homochiral PAHs, which combines carbohelicenes with non-planar PAHs containing non-hexagonal rings,[1][8] either pentagons in corannulene-helicene hybrid systems,[9] or heptagons in saddle-helix hybrid PAHs.[10] This strategy is growing interest since it enables the study of novel chiroptical properties that can emerge from the combination of twisted and curved aromatic surfaces in a single π-system.[11] Particularly, our research group has been interested in inducing circularly polarized luminescence (CPL) responses into graphene-type materials as they can be considered ideal candidates for many photonic technologies.[12]

Recently, we have presented the first family of CPL-active nanographenes,[10b-d] consisting on doubly distorted systems where negatively curved heptagon-containing HBCs are combined with carbo[n]helicenes. These structures are a prime example of π-extended helicenes, which lead to highly distorted homochiral helical nanographenes of different sizes and shapes, reaching values of g_{lum} up to 2×10^{-3}. At this point, we wondered if the introduction of a saddle-curved octagonal carbocycle as a constituent part of both the HBC core and the carbo[n]helicene, could lead to highly distorted HBCs with new rigid chiral motifs for CPL-response evaluation. In this way, we would present a new family of doubly distorted HBC-based helical nanographenes.[13]

Twisted octagon-containing PAHs have been reported as the [8]circulenes[14] and related laterally π-extended derivatives.[15] However, these nanostructures are usually quite flexible preventing their homochiral isolation. In this line, Mastalerz *et al.,* have recently demonstrated that monkey saddle structures can be isolated as homochiral PAHs with a racemization barrier of 24.4 kcal mol^{-1}.[16] Other remarkable related PAHs containing a cyclooctatetraene (COT) moiety incorporated into [5]helicenes[17] or [7]helicenes[18] (Figure 1c) have been reported leading to much more rigid structures (54 kcal mol^{-1} at 613 K) than simple carbo[5]helicene or even carbo[16]helicene.[19] Moreover, the inclusion of octagonal cores into helicenes has allowed Teply *et al*. to study the process of racemization of helicenes through saddle-shaped species.[20

Despite the impressive examples reported so far, to the best of our knowledge, there are no precedents of distorted HBCs units bearing an octagon-containing carbohelicene within their skeleton, although it would represent a new family of distorted nanographenes for future incorporation into novel superhelicenes. New highly distorted PAHs could lead to rigid schwarzite-like structures enabling their chiroptical study.

Herein, we present the synthesis, characterization and chiroptical properties of a new family of saddle-helix hybrid nanographenes (**1**-**3**) (Figure 1b), bearing a π-extended octagon-containing carbo[5]helicene (*oct-[5]helicene*) as an unprecedented chiral moiety. Novel structural features are

displayed by those highly distorted HBC analogues as well as remarkably high rigidity and interesting chiroptical responses.

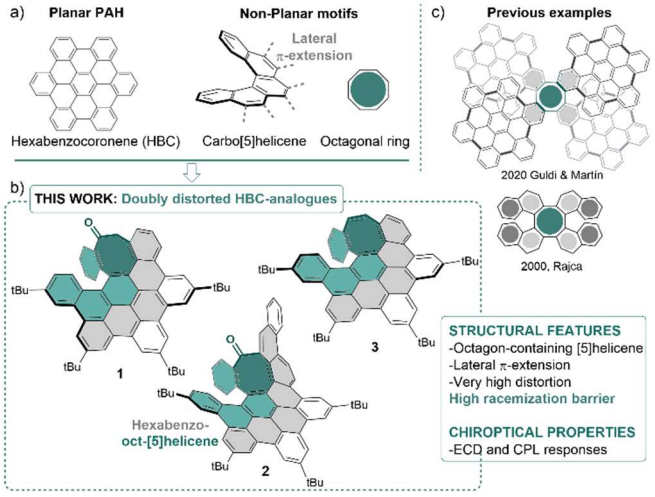

Figure 1. Schematic representation of the structural motifs combined (a) in the new distorted nanographenes presented in this work (b), and previous related examples (c).

Results and Discussion

Compounds **1-3** were prepared by the synthetic strategy depicted in Scheme 1 following the general approach used for nanographenes synthesis based on combining a Diels-Alder reaction to create a hexaphenylbenzene derivative and a subsequent oxidative cyclodehydrogenation reaction.[21] In this case, the key octagon-containing hexaphenylbenzene **6** (Scheme 1) was prepared from described dibenzocyclooctyne **4** and 2,3,4,5-tetrakis(4-*tert*-butylphenyl)-cyclopentadienone **5**. After a subsequent sequence of deprotection and oxidation, ketone **7** was isolated.

Encouraged by our previous results[22] and the pioneering work of Miao *et al.*,[23] where the oxidative cyclodehydrogenation reaction of heptagon-containing hexaphenylbenzene derivatives can lead to helical moieties, we envisioned that the insertion of a highly curved octagonal ring into the hexaphenylbenzene skeleton **7** might enable the formation of oct-helicene moieties in the final HBC unit. In this sense, the formation of oct-helicenes under Scholl-type reaction conditions was firstly suggested by Müllen, although, it was never confirmed or studied.[24] Pleasingly, oxidative cyclodehydrogenation of **7** by combining DDQ/CH_3SO_3H provided **1** selectively, although with moderate yield. None of the other possible carbohelicenes was obtained and the same selectivity was also observed by a $FeCl_3$-mediated oxidative dehydrogenative reaction (see ESI). In this case, the position of the carbonyl group is responsible for the regioselectivity observed, behaving as a deactivating group for an oxidative Scholl reaction.[25]

On the other hand, the reactivity of the ketone moiety allows easy further derivatizations. Firstly, we synthetized **2** by means of aldol condensation of **1** with 2-bromobenzaldehyde followed by Pd-mediated intramolecular arylation, leading to an additional π-extension of the *oct-[5]helicene* unit. Furthermore, a sequence of reduction and elimination from **1** leads to the all-carbon fully conjugated analogue **3** (Scheme 1).

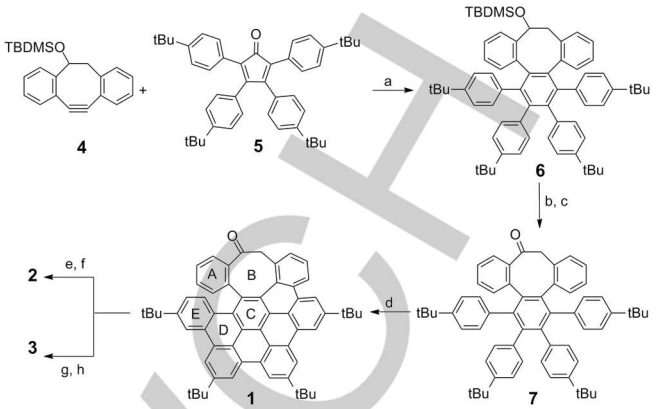

Scheme 1. Synthesis of **1-3**. Reagents and conditions: a) Ph_2O, reflux, 2 h, 91%; b) TBAF, THF, rt, 1 h, 93%; c) Dess-Martin periodinane, CH_2Cl_2, 0 ºC to rt, 4 h, 96%; d) DDQ, CF_3SO_3H, CH_2Cl_2, 0 °C, 10 min, 61%; e) 2-bromobenzaldehyde, NaH, THF, 60 ºC, 2 h, 55%; f) $Pd(OAc)_2$, K_2CO_3, SPhos, DMF, 135 ºC, 16 h, 55%; g) $NaBH_4$, CH_2Cl_2, rt, 2 h; h) H_2SO_4, toluene, 80 ºC, 5 min, 51%.

Due to their highly distorted skeletons, compounds **1-3** were very soluble in common organic solvents and, therefore, they could be fully characterized by means of ^{1}H- and ^{13}C-NMR spectroscopy and HRMS (see ESI, Figures S25-S43). Moreover, single crystals of **2** suitable for X-ray diffraction were grown by slow diffusion of acetonitrile into a chloroform solution of **2** followed by further slow evaporation at rt (Figure 2 middle and ESI, Figure S44). Thus, the structure of **2** was unambiguously determined by X-ray crystallography, revealing the deep saddle curvature caused by the octagonal moiety and the highly twisted π-extended oct-[5]helicene unit.

As shown in Figure S45, the saddle curvature reaches 2.71 Å deep and it is non-symmetrical due to helical moiety and the lateral π-extension on each side of the octagonal ring.

The π-extended *oct-[5]helicene* as novel helical unit (namely, hexabenzo-*oct-[5]helicene* moiety, colored in figure 2) resulted in an extremely distorted unit in comparison with previously reported carbo[5]helicenes. Thus, we found that the angle between the two planes of the terminal rings (Figure 2, middle, in orange) is exceptionally high (73.8º) when compared to pristine carbo[5]helicene (46º)[26] or even highly strained PAHs with a multiple hexapole [5]helicene (69º).[3b-c] Even comparing with Rajca's *oct-[5]helicene* (72.4º, Figure 1),[27] the terminal rings of **2** arranged more perpendicularly, showing the great influence of both the position of the octagonal ring in the helicene and the lateral π-extension in the distortion of the helical moiety (Fig. 2 middle, in gray). On the other hand, we found that the average torsion-angle of the *oct-[5]helicene* is 41.2°, much bigger than that observed for carbo[5]helicene[26] (9.1º) or even a multiple hexapole[5]helicene (21.8°).[3b-c] Furthermore, the maximal dihedral angle in the ring is 89.5°, being one of the largest angles reported so far for a carbo[5]helicene. Unfortunately, we were not able to obtain single crystals of **1** and **3**. Consequently, we carried out the geometrical optimization of **1-3** (DFT-CAM-B3LYP/6-31G(d,p)) and similar high distortion in the π-extended *oct-[5]helicene* moiety was observed in all cases (see ESI). Noteworthy, we observed remarkable good agreement between theoretical and X-ray crystal structures of compound **2**.

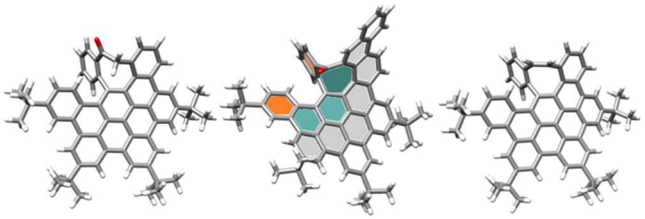

Figure 2. X-Ray crystal structure of **2** (middle) with hexabenzo-oct-[5]helicene highlighted in color. DFT optimized structures of **1** (left) and **3** (right). *M*-Enantiomers are shown. Color code: C (gray), O (red), H (white).

The optical and electronic properties of **1-3** were investigated by UV-Vis absorption and fluorescence spectroscopy, and cyclic voltammetry. As shown in Figure 3, absorption maxima of each compound (**1-3**) in CH_2Cl_2 (ca. 1.6×10^{-5} M) appeared at 352 nm (ε (6.1×10^4 M^{-1} cm^{-1}), with a shoulder at 385 nm, 430 nm, and 383 nm for **1**, **2** and **3**, respectively. The maxima absorption wavelengths are in the same range as those reported for hexakis-*tert*-butyl-HBC (tBu-HBC, λ_{max} = 359 nm)[7a] and red-shifted compared to [5]helicene (λ_{max} = 287 nm),[28] as expected from the extended conjugation in the π-structure, suggesting a higher energetic HOMO and lower oxidation potential. In fact, the absorption onset of compounds **1-3** (535 nm, 476 nm and 450 nm) corresponds to an optical band gap of 2.31 eV, 2.60 eV and 2.75 eV for **1**, **2** and **3**, respectively, lower than the ones reported for [5]helicene (350 nm; 3.54 eV),[29] or *t*Bu-HBC (2.8 eV).[7a]

We also studied the electrochemistry of **1-3**. Here, we found that the cyclic voltammogram of **2** in CH_2Cl_2 (ca. 6.1×10^{-4} M) shows one reversible oxidation and two reduction waves from 0.82 to -1.97 and -2.27 eV (*vs Fc/Fc*$^+$*;* see ESI, Figure S17). Therefore, from the first half-wave oxidation and reduction potentials we obtained a HOMO–LUMO gap of 2.79 eV, in good agreement with the obtained optical band gap. However, for compound **3**, we only found one reversible oxidation (see ESI, Figure S18), and, surprisingly, for **1** we could not observe any signal.

Solutions of HBC analogues **1-3** in CH_2Cl_2 resulted fluorescent after irradiation with UV light, with the maxima of the emission centered at 480, 538 and 460 nm (Figure 3), reaching fluorescence quantum yields (Φ_f) of 13%, 7% and 2%, respectively. Remarkably, the Φ_f of **1** is more than triple than the one reported for pristine [5]-helicene (4%) or *t*Bu-HBC (4%)[7a] with a very long lifetime (τ= 18 ns). Also **3** holds a very long lifetime (τ = 13 ns), which make them good candidates for bioapplications. In contrast, **2** holds a lower lifetime (τ= 4.5 ns), presumably due to a major flexibility than **1**, in agreement with the obtained non-radiative decay constants (**1** k_{nr} = 0.05 ns^{-1}; **2** k_{nr} = 0.21 ns^{-1} and **3** k_{nr} = 0.08 ns^{-1}).

Chiral resolution of *oct-[5]helicenes* **1-3** was attained by chiral stationary phase HPLC ((CSP)HPLC) (see ESI, Figures S1-S3), which showed that enantiopure compounds are reasonably rigid at room temperature as expected from their torsion angles and despite not being substituted in the fjord region. Furthermore, we determined the racemization barrier of **1-3** by following the enantiomeric excess decay over time at different temperatures (see ESI). While the energy barrier of **2** is slightly higher (24.9 kcal/mol) than the classic [5]-helicene (24.1 kcal/mol), we found that for **1** and **3**, neither racemization nor decomposition were observed by chiral HPLC after heating hexadecane solutions of each compound at 200 ºC for 5 h. On the other hand, the lowest racemization barrier of **2** could be presumably due to conformational changes around the additional π-extension surrounding the helicene moiety. In this sense, the isomerization could be favored by a process from twisted to saddle-shaped species.[22]

After racemic resolution, chiroptical properties were investigated by both electronic circular dichroism (ECD) and circularly polarized luminescence (CPL). The ECD spectra in dichloromethane (ca. 1.6×10^{-5} M) display mirror images for both enantiomers of each compound **1-3** with several opposite Cotton effects in the UV-Vis region up to 450 nm, which match with the corresponding UV-Vis spectra. First eluted fractions of each compound **1-3** presented a positive Cotton effect at their corresponding lowest energy band (Figure 3, middle/bottom, solid lines). For **1**, the first eluted fraction had two bands of major intensity with a positive Cotton effect at 258 nm ($|\Delta\varepsilon|$ =21.4 M^{-1} cm^{-1}, g_{abs} = 1.3×10^{-3}) and at 360 nm ($|\Delta\varepsilon|$ = 18.0 M^{-1} cm^{-1}, g_{abs} = 5.5×10^{-4}), respectively (see ESI, Figure S8). In the case of **2**, the most intense band at 295 nm ($|\Delta\varepsilon|$ = 42.2 M^{-1} cm^{-1}, g_{abs} = 1.5×10^{-3}) had an opposite Cotton effect compared to the band of longest wavelength at 427 nm ($|\Delta\varepsilon|$ = 25.1 M^{-1} cm^{-1}, g_{abs} = 6.7×10^{-4}). Finally, the first eluted peak of **3** showed a positive Cotton effect at the most intense band at 355 nm ($|\Delta\varepsilon|$ = 42.0 M^{-1} cm^{-1}, g_{abs} = 7.6×10^{-4}) (see ESI, Figure S10). Second eluted (CSP)HPLC fractions gave rise to the corresponding mirror images (see ESI, Figures S8-S10). These results show that the enantiomeric forms of **2** present higher chiroptical responses in terms of the dissymmetry factor (g_{abs}) than compounds **1** and **3** probably derived from the additional π-extension of the helical moiety. On the other hand, the g_{abs} values of **2** are more similar to that of (*P*)-(+)-[5]helicene (g_{abs} = $+4.2\times10^{-3}$).[30] The configurations of the six enantiomers were assigned by comparison of the experimental ECD with the TD-DFT simulated ECD spectra (see ESI, Figures S46-S51). In this sense, first (CSP)HPLC fractions were assigned to (*P*)-enantiomers and the second ones to (*M*)-enantiomers, thus, the sign of the ECD signal at the longest wavelength is consistent with that described for carbo[n]helicenes.[31]

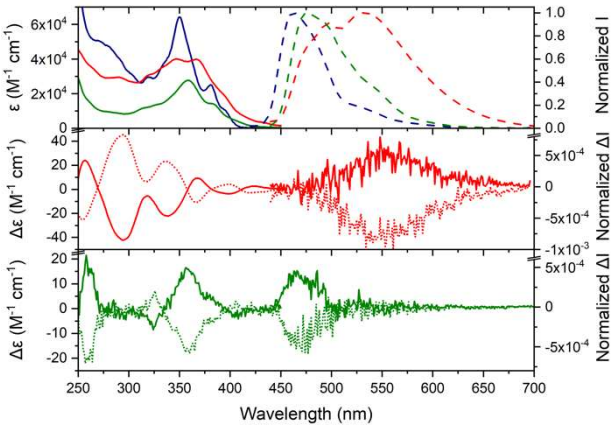

Figure 3. Top: UV-Vis absorption (solid line) and fluorescence spectra (dashed line) of **1** (green), **2** (red) and **3** (blue). Middle/Bottom: ECD (left, 250-450 nm) and CPL spectra (right, 450-700 nm) of **1** (bottom) and **2** (middle) in CH_2Cl_2 at rt. First, *P* (solid line) and second, *M* (dashed line) (CSP)HPLC eluted fractions.

Finally, as expected from chiral and emissive compounds, **1** and **2** are CPL-active, becoming part of the still exclusive family of CPL-emissive nanographenes.[10b-d] Unfortunately, for compound **3** we were not able to obtain the CPL spectra as it

decomposed under the long-time irradiation required for CPL (see ESI, Figure S43).[32] The CPL of each enantiomer was measured in dichloromethane (ca. 1.6×10^{-5} M), and the different enantiomeric forms gave CPL of opposite signs as expected for pure CPL without the presence of any artifacts[33] (Figure 3). Likewise, the signs of the CPL spectra were in all cases in good correlation with the signs of the longest wavelength ECD signal.[34] For the enantiomers of **1** (Figure 3, bottom right, from 450 nm, in green), the CPL spectra showed a maximum centered at 470 nm with a similar profile to the corresponding fluorescence spectrum and a g_{lum} value estimated as 4×10^{-4}. For the enantiomeric forms of **2**, the CPL maximum was centered at 554 nm (Figure 3, middle right, from 450 nm, in red) with a g_{lum} value of 7×10^{-4}. Remarkably, in this case, the profile does not fit with the corresponding fluorescence spectrum, which shows two peaks whereas in CPL spectra a single band centered at 550nm is observed. In order to investigate this phenomenon, we performed a Time Resolved Emission Spectra (TRES) analysis in the 400-720 nm range to obtain the deconvolution of the fluorescence spectrum into the different species. The analysis showed the presence of three lifetimes (Figure 4 top) with very different magnitude and area of the species-associated emission spectra (SAEMS). It was found that the species with the shortest lifetime (Figure 4, violet dots) is the main responsible of the shape of the fluorescence spectrum. Although this is the most abundant species, there are also two minor species in the excited state; one blue-shifted with a notably long lifetime of 17 ns (gray dots) and the other one, broader, and centered at 550 nm with a value of 4.5 ns (red dots). Comparing the shape and the maximum of the latter with the one obtained in the CPL experiment (Figure 4 down) we found they are essentially the same, suggesting that the CPL signal is associated only with this species.[35] The presence of different emissive species could be attributed to the π-extended *oct-[5]helicene* moiety, as the interconversion between conformers might be slower than the emission process.

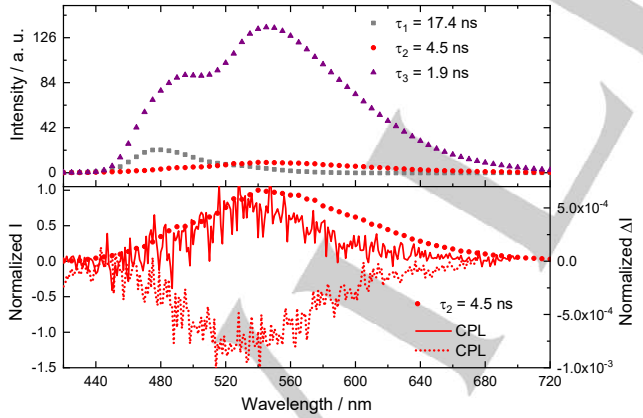

Figure 4. Top: SAEMS spectra of **2** in CH_2Cl_2 as solvent. Bottom: comparison of normalized CPL signal (red lines) of **2** and emission of the species corresponding to τ_2=4.5 ns (red dots) of **2** in CH_2Cl_2.

Conclusion

A new series of HBC analogues bearing highly twisted *oct-[5]helicenes* have been presented. The strategic insertion of an octagonal core into the formation of nanographenes leads to doubly and highly distorted π-extended [5]helicenes, which exhibit a very high isomerization barrier and interesting chiroptical properties. This family might open a new avenue of research toward highly twisted PAHs derivatives for molecular materials with desirable chiroptical properties, particularly as examples of saddle-helix hybrid nanographenes with a CPL-emission capability.

Acknowledgements

We acknowledge the European Research Council (ERC) under the European Union's Horizon 2020 research and innovation program (ERC-2015-STG-677023), the Ministerio de Ciencia, Innovación y Universidades (MICIU/FEDER/AEI, Spain, PGC2018-101181-B-I00) and Universidad de Granada (UGR) (Plan Propio - Intensificación de la Investigación PP2017-PRI.I-02) for financial support. We thank the CSIRC-Alhambra for supercomputing facilities. S. P. M. thanks the MINECO for the IJCI- 2017-31674.

Keywords: chirality • circularly polarized luminescence • helicenes • nanographenes • octagonal carbocycle

[1] S.H. Pun, Q. Miao, *Acc. Chem. Res.* **2018**, *51*, 1630–1642.

[2] M. Ball, Y. Zhong, Y. Wu, C. Schenck, F. Ng, M. Steigerwald, S. Xiao, C. Nuckolls, *Acc. Chem. Res.* **2015**, *48*, 267–276.

[3] a) T. Fujikawa, Y. Segawa, K. Itami, *J. Am. Chem. Soc.* **2015**, *137*, 7763–7768; b) T. Hosokawa, Y. Takahashi, T. Matsushima, S. Watanabe, S. Kikkawa, I. Azumaya, A. Tsurusaki, K. Kamikawa, *J. Am. Chem. Soc.* **2017**, *139*, 18512−18521; c) V. Berezhnaia, M. Roy, N. Vanthuyne, M. Villa, J.-V. Naubron, J. Rodriguez, Y. Coquerel, M. Gingras, *J. Am. Chem. Soc.* **2017**, *139*, 18508−18511; d) N. J. Schuster, R. Hernández Sánchez, D. Bukharina, N. A. Kotov, N. Berova, F. Ng, M. L. Steigerwald, C. Nuckolls, *J. Am. Chem. Soc.* **2018**, *140*, 6235–6239

[4] a) H. Isla, J. Crassous, *C. R. Chimie* **2016**, *19*, 39–49; b) Y. Yang, B. Rice, X. Shi, J. R. Brandt, R. Correa da Costa, G. J. Hedley, D.-M. Smilgies, J. M. Frost, I. D. W. Samuel, A. Otero-de-la-Roza, E. R. Johnson, K. E. Jelfs, J. Nelson, A. J. Campbell, M. J. Fuchter, *ACS Nano* **2017**, *11*, 8329−8338; c) Z. Ma, T. Winands, N. Liang, D. Meng, W. Jiang, N. L. Doltsinis, Z. Wang, *Sci. China Chem.* **2020,** *63*, 208–214.

[5] a) M. Rickhaus, M. Mayor, M. Juríček, *Chem. Soc. Rev.,* **2016**, *45*, 1542–1556; b) Y. Segawa, H. Ito, K. Itami, *Nat. Rev. Mater.* **2016**, *1*, 15002; c) M. Rickhaus, M. Mayor, M. Juríček, *Chem. Soc. Rev.* **2017**, *46*, 1643–1660; d) M. A. Majewski, M. Stępień, *Angew. Chem. Int. Ed.* **2019**, *58*, 86–116; *Angew. Chem.* **2019**, *131*, 90–122.

[6] a) Y. Nakakuki, T. Hirose, H. Sotome, H. Miyasaka, K. Matsuda, *J. Am. Chem. Soc.* **2018**, *140*, 4317−4326; b) Y. Zhu, Z. Xia, Z. Cai, Z. Yuan, N. Jiang, T. Li, Y. Wang, X. Guo, Z. Li, S. Ma, D. Zhong, Y. Li, J. Wang, *J. Am. Chem. Soc.* **2018**, *140*, 4222–4226; c) A. Bedi, L. J. W. Shimon, O. Gidron, *J. Am. Chem. Soc.* **2018**, *140*, 8086–8090; d) A. Bedi, O. Gidron, *Chem. Eur. J.* **2019**, *25*,3279 –3285; e) G. Liu, T. Koch, Y. Li, N. Doltsinis, Z. Wang, *Angew. Chem. Int. Ed.* **2019**, *58*,178–183; *Angew. Chem.* **2019**, *131*, 184–189; f) Y. Hu, G. M. Paterno, X. Y. Wang, X.–C. Wang, M. Guizzardi, Q. Chen, D. Schollmeyer, X.–Y. Cao, G. Cerullo, F. Scotognella, K. Müllen, A. Narita, *J. Am. Chem. Soc.* **2019**, *141*, 12797–12803; g) M. Roy, V. Berezhnaia, M. Villa, N. Vanthuyne, M. Giorgi, J.-V.Naubron, S. Poyer, V. Monnier, L. Charles, Y. Carissan, D. Hagebaum-Reignier, J. Rodriguez, M. Gingras, Y. Coquerel, *Angew. Chem. Int. Ed.* **2020**, *59*, 3264–3271; *Angew. Chem.* **2020**, *132*, 3290–3297.

[7] a) D. Reger, P. Haines, F. W. Heinemann, D. M. Guldi, N. Jux, *Angew. Chem. Int. Ed.* 2018, 57, 5938–5942; *Angew. Chem.* **2018**, 130, 6044–6049; b) P. J. Evans, J. Ouyang, L. Favereau, J. Crassous, I. Fernández, J. Perles, N. Martín, *Angew. Chem., Int. Ed.* **2018**, 57, 6774−6779; *Angew. Chem.*, **2018**, 130, 6890–6895; c) Y. Zhu, X. Guo, Y. Li, J. Wang, *J. Am. Chem. Soc.* **2019**, *141*, 5511−5517.

[8] a) I. R. Márquez, S. Castro-Fernández, A. Millán, A. G. Campaña, *Chem. Commun*. **2018**, *54*, 6705–6718; b) E. M. Muzammil, D. Halilovic, M. C. Stuparu, *Commun. Chem.* **2019**, *2*, 58.

[9] a) M. Yanney, F.R. Fronczek, W. P. Henry, D.J. Beard, A. Sygula, *Eur. J. Org. Chem.* **2011**, 6636–6639, b) K. Kato, Y. Segawa, L. T. Scott, K. Itami, *Angew. Chem. Int. Ed.***2018**, *57*, 1337–1341; *Angew. Chem.* **2018**,*130*, 1351–1355; c) J. M. Fernández-García, P. J. Evans, S. Medina Rivero, I. Fernández, D. García-Fresnadillo, J. Perles, J. Casado, N. Martín, *J. Am. Chem. Soc.* **2018**, *140*, 17188–17196; d) D. Meng, G. Liu, C. Xiao, Y. Shi, L. Zhang, L. Jiang, K. K. Baldridge, Y. Li, J. S. Siegel, Z. Wang, *J. Am. Chem. Soc.* **2019**, *141*, 5402–5408.

[10] a) T. Fujikawa, Y. Segawa, K. Itami, *J. Org. Chem.* **2017**, *82*, 7745−7749; b) C. M. Cruz, I. R. Márquez, I. F. A. Mariz, V. Blanco, C. Sánchez-Sánchez, J. M. Sobrado, J. A. Martín-Gago, J. M. Cuerva, E. Maçôas, A. G. Campaña, *Chem. Sci.* **2018**, *9*, 3917–3924; c) C. M. Cruz, S. Castro-Fernández, E. Maçôas, J. M. Cuerva, A. G. Campaña, *Angew. Chem. Int. Ed.* **2018**, *57*, 14782–14786; *Angew. Chem.* **2018**, *130,* 14998–15002; d) C. M. Cruz, I. R. Márquez, S. Castro-Fernández, J. M. Cuerva, E. Maçôas, A. G. Campaña, *Angew. Chem. Int. Ed.* **2019**, *58*, 8068–8072; *Angew. Chem.* **2019**, *130,* 8152–8156; e) J. Ma, Y. Fu, E. Dmitrieva, F. Liu, H. Komber, F. Hennersdorf, A. A. Popov, J. J. Weigand, J. Liu, X. Feng, *Angew. Chem. Int. Ed.* **2020**, *59*, 5637–5642; *Angew. Chem.* **2020**, *132*, 5686–5691.

[11] C. M. Cruz, S. Castro-Fernández, E. Maçôas, A. Millán, *A. G. Campaña*, *Synlett* **2019**, *30*, 997–1002.

[12] a) Y. Yang, R.C. da Costa, M. J. Fuchter, A. J. Campbell, *Nat. Photonics* **2013**, *7*, 634–638; b) H. Tanaka, M. Ikenosako, Y. Kato, M. Fujiki, Y. Inoue, T. Mori, *Commun. Chem.* **2018**, *1,* 38–45; c) W.-L. Zhao, H.-Y. Lu, C.-F. Chen, *Chem. Commun.* **2019**, *55*, 13793–13803.

[13] M. M. Matin, F. Hampe, N. Jux, *Chem. Eur. J.* **2019**, *25*, 15083–15090.

[14] a) Y. Sakamoto, T. Suzuki, *J. Am. Chem. Soc.* **2013**, *135*, 14074–14077; b) R. W. Miller, A. K. Duncan, S. T. Schneebeli, D. L. Gray, A. C. Whalley, *Chem. Eur. J.* **2014**, *20*, 3705–3711.

[15] a) K. Y. Cheung, C. K. Chan, Z. Liu, Q. Miao, *Angew. Chem. Int. Ed.* **2017**, *56*, 9003–9007; *Angew. Chem.* **2017**, *129*, 9131–9135; b) S. H. Pun, Y. Wang, M. Chu, C. K. Chan, Y. Li, Z. Liu, Q. Miao, *J. Am. Chem. Soc.* **2019**, *141*, 9680−9686.

[16] T. Kirschbaum, F. Rominger, M. Mastalerz, *Angew. Chem. Int. Ed.* **2019**, *59, 270–274; Angew. Chem.* ***2020****, 132, 276–280.*

[17] A. Rajca, A. Safronov, S. Rajca, J. Wongsriratanakul, *J. Am. Chem. Soc.* **2000**, *122*, 3351–3357.

[18] J. Urieta-Mora, M. Krug, W. Alex, J. Perles, I. Fernández, A. Molina-Ontoria, D. M. Guldi, N. Martín, *J.* Am. Chem. Soc. **2020**, *142*, 4162–4172.

[19] J. Barroso; J. L. Cabellos, S. Pan, F. Murillo, X. Zarate, M. A. Fernandez-Herrera, G. Merino, *Chem. Commun*. **2018**, *54*, 188–191.

[20] L. Adriaenssens, L. Severa, D. Koval, I. Císarová, M. Martínez Belmonte, E. C. Escudero-Adán, P. Novotná, P. Sázelová, J. Vávra, R. Pohl, D. Saman, Marie Urbanová, V.Kasickaa, F. Teply, *Chem. Sci.* **2011**, *2*, 2314–2320.

[21] M. Müller, C. Kübel, K. Müllen, *Chem. Eur. J.* **1998**, *4*, 2099–2109.

[22] I. R. Marquez, N. Fuentes, C. M. Cruz, V. Puente-Munoz, L. Sotorrios, M. Luisa Marcos, D. Choquesillo-Lazarte, B. Biel, L. Crovetto, E. Gomez-Bengoa, M. T. Gonzalez, R. Martin, J. M. Cuerva, A. G. Campaña, *Chem. Sci.* **2017**, *8*, 1068–1074.

[23] J. Luo, X. Xu, R. Mao, Q. Miao, *J. Am. Chem. Soc*. **2012**, *134*, 13796−13803.

[24] M. Müller, V. S. Iyer, C. Kübel V. Enkelmann, K. Müllen, *Angew. Chem. Int. Ed.* **1997**, 36, 1607–1610; *Angew. Chem.***1997**, *109*, 1679–1682.

[25] M. Grzybowski, B. Sadowski, H. Butenschön, D. T. Gryko, *Angew. Chem. Int. Ed.* **2020**, *59*, 2998–3027; *Angew. Chem.* **2020**, *132*, 3020–3050.

[26] R. J. Kuroda, *J. Chem. Soc., Perkin Trans. 2* **1982**, *7*, 789−794.

[27] T. B. Freedman, X. Cao, A. Rajca, H.Wang, L. A. Nafie, *J. Phys. Chem. A* **2003**, *107*, 7692–7696.

[28] E. Clar, D. G. Stewart, *J. Am. Chem. Soc*. **1952**, *74*, 6235−6238.

[29] A.-C. BØdard, A. Vlassova, A. C. Hernandez-Perez, A. Bessette, G. Shanan, M. A. Heuft, S. K. Collins, *Chem. Eur. J.* **2013**, *19*, 16295−16302.

[30] Y. Nakai, T. Mori, Y. Inoue, *J. Phys. Chem. A* **2012**, *116*, 7372−7385.

[31] F. Furche, R. Ahlrichs, C. Wachsmann, E. Weber, A. Sobanski, F. Vögtle, S. Grimme, *J. Am. Chem. Soc.* **2000**, *122*, 1717–1724.

[32] Although the time of complete decomposition was determinated as 24 h, decomposition starts to appear after 2 h, which is time enough for studying the experimental ECD (see ESI, Figure S43), but not for measuring CPL.

[33] a) H. P. J. M. Dekkers, P. F. Moraal, J. M. Timper, J. P. Riehl, *Appl. Spectrosc.* **1985**, *39*, 818–821; b) J. P. Riehl, F. S. Richardson, *Chem. Rev.* **1986**, *86*, 1–16.

[34] H. Tanka, Y. Inoue, T. Mori, *ChemPhotoChem* **2018**, *2*, 386–402.

[35] P. Reiné, A. M. Ortuño, S. Resa, L. Álvarez de Cienfuegos, V. Blanco, M. J. Ruedas-Rama, G. Mazzeo, S. Abbate, A. Lucotti, M. Tommasini, S. Guisán-Ceinos, M. Ribagorda, A. G. Campaña, A. Mota, G. Longhi, D. Miguel, J. M. Cuerva, *Chem. Commun.,* **2018**, *54,* 13985–13988.

Entry for the Table of Contents

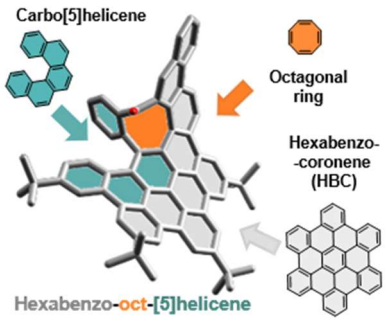

π-Extended oct-[5]helicene as novel helical unit: A new family of saddle-helix hybrid nanographenes is presented as chiral and emissive compounds that become part of the still exclusive family of CPL-emissive nanographenes.

Institute and/or researcher Twitter usernames: @canalUGR, @Campana_Lab, @SaraPMorcillo, @VBlanco_Chem, @PPhotobiology.